國立臺灣大學理學院地質科學系暨研究所

碩士論文

Institute of Geosciences

College of Sciences

National Taiwan University

Master Thesis

國立臺灣大學碩士畢業論文

National Taiwan University (NTU) Thesis

陳季晴

Ji Ching Chen

指導教授: 譚諤 博士

Advisor: Eh Tan Ph.D.

中華民國 111 年 5 月

May, 2022

doi:10.5566/NTU2018XXXXX

國立臺灣大學碩士學位論文
口試委員會審定書

國立臺灣大學碩士畢業論文

National Taiwan University (NTU) Thesis

本論文係陳季晴君（R09224122）在國立臺灣大學地質科學系暨研究所完成之碩士學位論文，於民國 111 年 5 月 1 日承下列考試委員審查通過及口試及格，特此證明

口試委員：＿＿＿＿＿＿＿＿＿＿＿＿＿＿＿＿＿＿＿＿

（指導教授）

所　　長：＿＿＿＿＿＿＿＿＿＿＿＿＿＿＿＿

doi:10.5566/NTU2018XXXXX

doi:10.5566/NTU2018XXXXX

Acknowledgements

還沒有

doi:10.5566/NTU2018XXXXX

doi:10.5566/NTU2018XXXXX

摘要

中文摘要

關鍵字： LaTeX、中文、論文、模板

doi:10.5566/NTU2018XXXXX

doi:10.5566/NTU2018XXXXX

Abstract

Abstract

Keywords: LaTeX, CJK, Thesis, Template

doi:10.5566/NTU2018XXXXX

doi:10.5566/NTU2018XXXXX

Contents

doi:10.5566/NTU2018XXXXX

doi:10.5566/NTU2018XXXXX

doi:10.5566/NTU2018XXXXX

doi:10.5566/NTU2018XXXXX

List of Figures

doi:10.5566/NTU2018XXXXX

doi:10.5566/NTU2018XXXXX

List of Tables

doi:10.5566/NTU2018XXXXX

doi:10.5566/NTU2018XXXXX

Denotation

E	能量
m	質量
c	光速
P	概率
T	時間
v	速度
勸學	君子曰

doi:10.5566/NTU2018XXXXX

doi:10.5566/NTU2018XXXXX

Chapter 1　Introduction

1.1　Background

在 1960 年代之前，地槽學說在大地構造學說中佔主要地位，該學說認為地殼運動方式以垂直運動為主，各個地殼區域內發生沈積與風化、岩漿活動、變質作用等運動。1967 年板塊構造學說提出，建立在大陸漂移與海底擴張等水平移動證據，打破以往地槽學說所認為的垂直運動概念。板塊構造學說首先定義地球最外熱邊界層以上剛性殼體—岩石圈。岩石圈包含地殼以及上部地幔，其因地球內部的熱引起重力不穩定而在軟流圈上水平運動 (Jordan, 1978)。地球的岩石圈斷裂成許多剛性塊體，該塊體被稱為板塊。大部分由板塊水平運動所引起的變形作用發生在板塊邊界。在聚合板塊邊界，板塊發生破壞，包含碰撞與隱沒; 在分離板塊邊界，板塊發生增生，代表構造為海底擴張；錯動邊界中板塊不會顯著發生增生與破壞，代表構造為轉型斷層 (Fowler, 2005)。全球主要的板塊邊界見圖 1-1。

聚合板塊邊界中，老的岩石圈因溫度較低使其密度相較於高溫地幔岩石圈更高，足夠造成重力不穩定。因此，老岩石圈在聚合板塊邊界發育海溝的，由海溝沉入地球內部，成為隱沒板塊。隨著隱沒板塊帶著較冷物質進入地幔深處，周圍壓力逐漸上升，岩石發生相變，隱沒板塊因成分與溫度與地幔物質不同，溫度上的差異造成更大的重力不穩定。在同等深度下，隱沒板塊的密度始終比周圍地幔高，為了隱沒系統的平衡，隱沒板塊持續下沉進入地球內部更深處，整段不穩定區域稱為隱沒帶不穩定。同時，隱沒板塊上的聚合板塊稱為上覆板塊。隱沒板塊為板塊移動與張裂的主要驅動力 (Turcotte and Schubert, 2002)，在隱沒過程中，岩

doi:10.5566/NTU2018XXXXX

石圈物質與軟流圈物質發生交互作用，隱沒板塊將海水與沈積物進入地幔中，降低地幔熔點，在上覆板塊側發生岩漿作用。自然界中上部地幔以上之隱沒幾何剖面有相當大的相異性，有許多原因影響隱沒傾角與隱沒曲率 (Schellart, 2020)。平坦隱沒是隱沒帶幾何中一種特殊的現象。在平坦隱沒的區域，有一部分的隱沒板塊在上覆板塊下方呈現接近水平走向的狀態一段距離後，又以正常隱沒傾角進入地幔深處。

大部分活躍的隱沒帶中，若僅考慮地表至 200 公里深的幾何構造，隱沒板塊的轉樞點接近海溝且下凹，並且只有一個轉樞點，如圖 1-2 (A)(B)。在部分區域，板塊會有兩個下凹轉樞點，第一個轉樞點接近海溝且呈現平緩不明顯的下凹，第二個轉樞點在距海溝幾百公里遠處，曲率明顯、板塊下凹進入深部地幔，如圖 1-2(C) 所示，阿拉斯加、卡斯卡迪亞 (Cascadia)、日本四國與新幾內亞等地區皆屬於此類。

另外在少數區域，隱沒板塊會有三個轉樞點，第一個轉樞點靠近海溝且下凹，第二個轉樞點深度較深呈現上凹，被視為是平坦隱沒的開始端，在這兩個轉樞點中隱沒板塊傾角正常。第三個轉樞點與第二個轉樞點深度相近，水平距離通常超過 100 公里以上，其曲率下凹的特徵代表著平坦隱沒的結束，平坦隱沒的距離與深度由第二與第三轉樞點所決定，如圖 1-2(D) 所示，智利、秘魯與墨西哥等地區屬於此類，在過去曾經被 Manea et al., 2017 所討論。在本研究中，平坦隱沒被定義為具有三個轉樞點的隱沒板塊。

doi:10.5566/NTU2018XXXXX

1.2 Review of flat subduction numerical models

目前造成平坦隱沒發生的機制眾說紛紜。南美洲區域平坦隱沒的發生區域與隱沒的中洋脊有幾何上的相關性，海洋地殼上中洋脊與海洋高原的存在可能會導致總體密度較低、浮力較大，因此過去曾經隱沒的中洋脊被認為是造成平坦隱沒的主要原因。

Hunen et al., 2002 最早將模型加入增厚的海洋地殼，以模擬過去智利與秘魯曾經有中洋脊與海洋高原進入隱沒帶中的紀錄。增厚海洋地殼有較低的密度與較大的浮力，其上方岩相需要比原先更大的壓力與更高的溫度才會從玄武岩相變成密度高的榴輝岩，可能使隱沒板塊與周遭地幔沒有顯著密度差而發生平坦隱沒。不過由於該研究模型僅二維，單純加入增厚海洋地殼所呈現的模型雖然能呈現平坦隱沒，但結果是假設第三維上有無限延伸的增厚海洋地殼，現實中增厚的海洋地殼能造成的浮力效應應遠小於二維模型中的結果。Florez-Rodr´ıguez et al., 2019 在三維模型中證明了這一點，他們提出若將現在自然界中最大的洋脊隱沒進入地幔，其所提供的浮力也只會造成海洋板塊傾角減少原先的 10 度。若從自然界中來看，確實有許多區域皆有海脊隱沒的證據，例如勘察加半島 (Kamchatka) 有皇帝海脊 (Emperor Ridge) 隱沒、琉球 (Ryukyu) 有大東海脊 (Daito Ridge) 隱沒以及馬里亞納 (Mariana) 與馬庫斯—內克海脊 (Marcus-Necker Ridge) 隱沒，然而只有秘魯與智利有平坦隱沒的特徵。此外，在墨西哥有平坦隱沒的特徵，然而墨西哥沒有任何海脊或海洋高原的隱沒紀錄，因此增厚的海洋地殼發生平坦隱沒的理論近年來逐漸站不住腳 (Schellart, 2020)。

Hunen et al., 2000 使用二維笛卡爾座標數值模型進行祕魯與智利平坦隱沒的模擬。在他們得模型中，唯一能成功演化出平坦隱沒的機制只有海溝後撤迫使大陸

doi:10.5566/NTU2018XXXXX

岩石圈逆衝到隱沒板塊之上。Liu and Currie, 2016 使用二維模型模擬過去股法拉隆板塊板塊的平坦隱沒機制，他們加入增厚的海洋地殼後並無法觸發平坦隱沒的產生，然而，再加入額外大陸岩石圈的水平速度後，平坦隱沒便能成功再現。Axen et al., 2018 使用同樣的數值模型將古代北美西部的克拉通放置於大陸板塊測，成功模擬出增厚海洋地殼加上快速移動大陸岩石圈能發生平坦隱沒，並且能將克拉通從大陸岩石圈底部刮除，證實了平坦隱沒能破壞大陸岩石圈。在該研究中並沒有考慮克拉通對平坦隱沒的影響。

Manea et al., 2012 提出了另外的看法。他們利用三維模型模擬過去 30Ma 以來智利區域的隱沒帶動態行為，使用額外施加的邊界條件強迫智利海溝後撤，發現海溝後撤能夠施加給隱沒板塊的地幔流吸力 (suction) 不足以讓巨大厚重的海洋板塊變平坦，因此他們在模型上覆板塊加上克拉通，系統性測試從 150-300 公里厚的大陸岩石圈與海溝距離 600-1000 公里時隱沒帶下方地幔流產生的動力壓力 (dynamic pressure)。他們發現在只有在克拉通與海溝距離約 800 公里且克拉通厚度大於 200 公里時平坦隱沒才會生成。當他們把造成海溝後撤的邊界力移除時，不會觸發平坦隱沒的形成，因此他們得出的結論是需要同時有海溝後撤與克拉通的存在才會觸發平坦隱沒。這是首次將克拉通加進數值模型裡的平坦隱沒模型。隨後 Liu and Currie, 2016 效仿同樣的機制，將過去普遍認為存在於北美板塊西部下方的科羅拉多高原山根放入模型中，模擬古法拉龍板塊平坦隱沒演化。他們認為克拉通與山根的存在只是加快平坦隱沒的形成，但真正觸發平坦隱沒的機制是增厚海洋地殼延緩玄武岩相變成榴輝岩。Hu et al., 2016 使用三維模型 CitcomS 模擬整個南美洲海溝 45 Ma 以來隱沒帶演化。在加入克拉通的模型中，隱沒板塊傾角有降低的趨勢，不過根據模型結果，真正造成平坦隱沒的形成依然與隱沒海脊相關，只有在海脊進入三維模型後隱沒傾角才出現顯著降低。

doi:10.5566/NTU2018XXXXX

因此，目前的平坦隱沒數值模型大多以擬合智利、祕魯與法拉龍板塊為主，觸發平坦隱沒的機制大多與克拉通的存在與否、是否有洋脊隱沒以及上覆板塊的移動速度為主要測試，墨西哥區域尚未有平坦隱沒的數值模型被提出。在墨西哥，隱沒板塊上沒有任何增厚的紀錄，此外該地區北美板塊移動速率遠低於南美洲與過去法拉龍板塊隱沒時期的北美板塊，因此墨西哥區域的平坦隱沒機制尚未有統一定論。本研究期待能利用數值模擬得到墨西哥平坦隱沒從過去 50 Ma 以來的演化，並提出新的演化機制模型，填補過去尚未成熟的平坦隱沒機制理論。

1.3 Movation

(尚未開始撰寫)

1.4 Geophysical observation in Cocos subduction zone

Pardo et al. 1995 最早藉由重新定位當地地震跟遠震判斷在墨西哥中部的板塊交界處下方有平坦隱沒存在。Pe´rez-Campos et al. 2008 使用接收函數得到平坦隱沒的影像 (圖 1-3) 。這是人類第一次看到隱沒板塊水平貼在大陸地殼下方呈水平走向隱沒，在平坦隱沒板塊段與大陸板塊交界處中，初步判斷只有不到三公里厚的地幔岩石圈，該範圍屬於誤差區間，目前還無法判斷隱沒板塊是貼著上覆大陸地殼或中間夾帶大陸地幔成分。

在 Cocos plate 上方由地震波研究證明 (Song et al. 2009) 被認為有一層 Vs 低速層，Song 2009, Song 2012, Kim 2012 都認為該低速層是由 oceanic slab 上的物質所組成，而早先時候 Pe´rez-Campos et al. 2008 接收函數同樣有看到低速層 (圖 1-3)，

doi:10.5566/NTU2018XXXXX

但沒有特別針對該層多做解釋。Song 2009 猜測是蛇紋岩與高孔隙水壓。因板塊交界有一層低速層的關係，被認為兩個板塊耦合低 (decoupled)。Manea et al. 2013 認為這層低速成是由蛇紋岩所造成，由於 Cocos plate 隱沒時的年紀輕，地溫梯度較高，水大約在 50-70 km 就會釋出，導致部分地幔被蛇紋岩化。

在一個隱沒帶中，通常會把隱沒板塊區分成幾段探討中間的耦合機制，區分辨法都以溫度當作約束。在大約 150 度到 350 度是地震會發生的地方，稱作 seismogenic zone，150 度之前會有大量水份從沉積物釋放，所以介面多以滑動為主，在 150 度後因為水份已經消失，使板塊介面變成鎖住的狀態，因此許多地震會在這裡發生 Manea et al. 2013 認為 seismogenic zone 大約在 150-300 度之間。到了 350-450 度之間，因為溫度過高開始產生變質相變，出現蛇紋岩，因此板塊介面又轉為弱耦合，以滑動為主。從上述的溫度約束可以判斷，當年輕板塊隱沒時，板塊傾角較低，150-300 度的介面面積會相對很大，這時候鎖住區很遠很大，會產生較大的地震規模事件。不過在墨西哥區域並沒有在內陸發生大規模地震是件的紀錄，因此在平坦隱沒區域中，可能有其他機制主導隱沒板塊與上覆板塊之間的耦合現象。(尚未完成，待補)

1.5 End

(尚未開始撰寫)

doi:10.5566/NTU2018XXXXX

Chapter 2 Numerical modelling method

Since the subduction process contain slow deformation and the constrain for deep lithosphere evolution is not well understand from either geophysical observation in depth or geology study in time, computer model is a suitable way to study subduction zone, especially the numerical model. While the analytic solution is hard to solve, numerical model has become a useful method for studying Earth evolution.

The numerical models in this study address the dynamics process of flat subduction, in which an oceanic plate subducts beneath continental plate. The goal of this work is to address the controls on subducting plate dynamics and to determine the conditions under which flat subduction may develop.

In this chapter, we introduce the method of numerical model and the initial model setup. In section 2.1, we discuss the governing equations. In section 2.2, the finite elements method will be briefly discuss. In section 2.3, we introduce the Fast Lagrangian Analysis of Continua technique. In section 2.4, the model geometry is presented. The material properties, phase transition and model boundary conditions are given in section 2.5 ,2.6 and 2.7, respectively.

2.1 Governing equation

2.1.1 Continuum—Conservation of mass

In geodynamics modelling, we consider major rock units as continuous geological media. The continuous description is described by field variables such as density, pressure, velocity, strain, etc. The continuity can be transformed into quantitative mathenatical formalism, that is, continuity equation.

The mass conservation equation in Lagrangian form is as follow

$$\frac{\partial \sigma_{ij}}{\partial x_j} + \rho g_i = \rho \frac{\partial D_{vi}}{\partial t} \tag{2.1}$$

A Lagrangian points is strictly connected to a single material point and is moving with this point. Therefore, the same material point is always in same coordinate independent of the moment of time. On the other hand, Eulerian point is an immobile point. The proof of eq.(2.1) is as follow

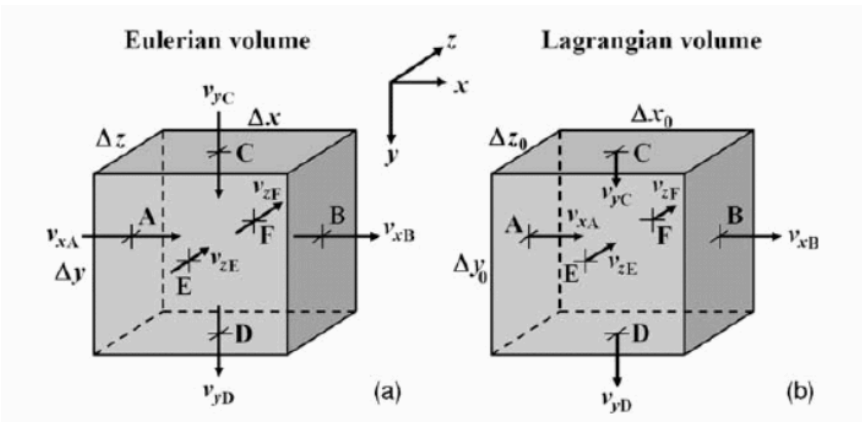

Figure 2.1: Eulerian (a) and Lagrangian (b) elementary volumes considered for the derivation of continuity equation.

doi:10.5566/NTU2018XXXXX

Since the volume is always related to the same material points, the amount of mass in the moving Lagrangian volume remains constant. However, the volume change due to the internal expansion or contraction process. The initial average density ρ_0 in a Lagrangian volume (V_0) is given by:

$$\rho_0 = \frac{m}{\Delta x_0 \Delta y_0 \Delta z_0} \tag{2.2}$$

After a small period of time (Δt), the Lagrangian volume undergo internal process, thus the volume become V_1 and the average density change to:

$$\rho_1 = \frac{m}{\Delta x_1 \Delta y_1 \Delta z_1} \tag{2.3}$$

Lagrangian material in time derivative is:

$$\frac{D\rho}{Dt} \approx \frac{\Delta \rho}{\Delta t} = \frac{\rho_1 - \rho_0}{\Delta t} = \frac{m}{\Delta x_1 \Delta y_1 \Delta z_1 \Delta t} - \frac{m}{\Delta x_0 \Delta y_0 \Delta z_0 \Delta t} \tag{2.4}$$

The relationship between new and old dimensions of Lagrangian volume is base on the relative movements of the volume's boundary, the displacement is equal to the velocity times duration period:

$$\Delta x_1 = \Delta x_0 + \Delta t \Delta v_x \tag{2.5}$$

$$\Delta y_1 = \Delta y_0 + \Delta t \Delta v_y \tag{2.6}$$

$$\Delta z_1 = \Delta z_0 + \Delta t \Delta v_z \tag{2.7}$$

doi:10.5566/NTU2018XXXXX

By using the equation above (2.5-2.7), replace the Δx_1, Δy_1, Δz_1 to eq 2.4:

$$\frac{D\rho}{Dt} \approx \frac{\Delta\rho}{\Delta t} = \frac{m\Delta x_0\Delta y_0\Delta z_0 - m\Delta x_1\Delta y_1\Delta z_1}{\Delta x_1\Delta y_1\Delta z_1\Delta t\Delta x_0\Delta y_0\Delta z_0} \tag{2.8}$$

Since $\Delta x_0\Delta y_0\Delta z_0 = \rho_0$, the following expression can be obtain:

$$\frac{\Delta\rho}{\Delta t} + \rho_0\frac{\frac{\Delta v_x}{\Delta x_0} + \frac{\Delta v_y}{\Delta y_0} + \frac{\Delta v_z}{\Delta z_0} + K_1}{K_2} = 0 \tag{2.9}$$

$$K_1 = \Delta t(\frac{\Delta v_x}{\Delta x_0}\frac{\Delta v_y}{\Delta y_0} + \frac{\Delta v_x}{\Delta x_0}\frac{\Delta v_z}{\Delta z_0} + \frac{\Delta v_y}{\Delta y_0}\frac{\Delta v_z}{\Delta z_0} + \Delta t\frac{\Delta v_x}{\Delta x_0}\frac{\Delta v_y}{\Delta y_0}\frac{\Delta v_z}{\Delta z_0}) \tag{2.10}$$

$$K_2 = (1 + \Delta t\frac{\Delta v_x}{\Delta x_0})(1 + \Delta t\frac{\Delta v_y}{\Delta y_0})(1 + \Delta t\frac{\Delta v_z}{\Delta z_0}) \tag{2.11}$$

where K_1 and K_2 are coefficients which respectively tend to zero and unity when Δt tends to zero. Eq (2.9) can be rewrite to:

$$\frac{D\rho}{Dt} + \rho\frac{\partial v_x}{\partial x} + \rho\frac{\partial v_y}{\partial y} + \rho\frac{\partial v_z}{\partial z} = 0 \tag{2.12}$$

or

$$\frac{D\rho}{Dt} + \rho div(\vec{v}) = 0 \tag{2.13}$$

While in geodynamics modelling, the density variations are small enough to be ignored, which is the result of Boussinesq approximation. The Boussinesq approximation assume that the density is linear proportional to the temperature and the small density

doi:10.5566/NTU2018XXXXX

variation is then neglected, except the gravity term.

$$\rho(T) = \rho_0[1 - \alpha(T - T_0)] \tag{2.14}$$

where ρ_0 is the reference density at temperature T_0 and α is the volumetric thermal expansion coefficient. The boussinesq approximation also represent the incompressible condition, which mean the density of material points does no change with time. The incompressible continuity equation is broadly used in numerical geodynamic modelling, although on many cases it is rather big simplification.

$$\nabla \cdot (\vec{v}) = 0 \tag{2.15}$$

Eq. (2.15) is the conservation of mass in our numerical modelling approach.

2.1.2 Motion—Conservation of momentum

In geodynamics, the time-dependent phenomena involve deformation of continuous media, which is the effect of the balance of internal and external forces that act in these media. So as to relate forces and deformation, an equation of motion may be used –The momentum equation. The momentum equation is a differential equivalent of Newton' s second law to a continuous medium.

$$f = ma \tag{2.16}$$

doi:10.5566/NTU2018XXXXX

f is the net force acting on the object and m is the mass of material. The momentum equation for a continuous medium in the gravity field: Eulerian Form:

$$\frac{\partial \sigma_{ij}}{\partial x_j} + \rho g_i = \rho(\frac{\partial v_i}{\partial t} + v_j \frac{\partial v_i}{\partial x_j}) \tag{2.17}$$

Lagrangian Form:

$$\frac{\partial \sigma_{ij}}{\partial x_j} + \rho g_i = \rho \frac{\partial D_{vi}}{\partial t} \tag{2.18}$$

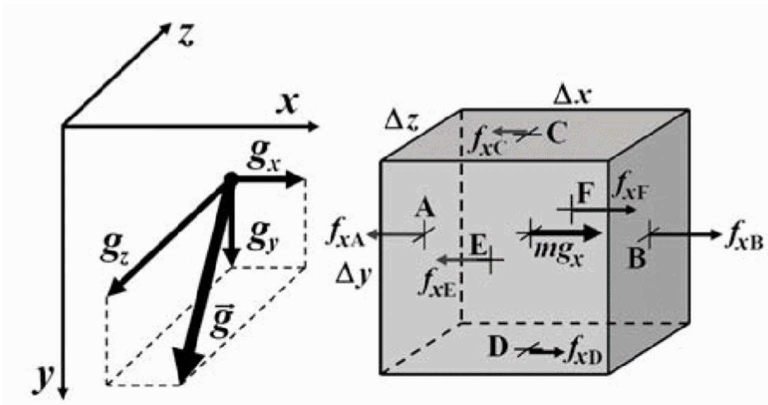

Figure 2.2: Lagrangian elementary Volume considered for the derivation of the respective form of x-momentum equation.

While considering a small Lagrangian volume, the net force acting on the object which can be computed locally. We will proof the momentum equation of Lagrangian Form below:

For x-component

$$f_x = f_{xA} + f_{xB} + f_{xC} + f_{xD} + f_{xE} + f_{xF} + mg_x \tag{2.19}$$

$f_{xA} - f_{xF}$ are stress-related forces, from the outside of the volume on the respective bound-

doi:10.5566/NTU2018XXXXX

aries A-F. $f_g = m_g x$ is the gravity force.

$$f_{xA} = -\sigma_{xxA}\Delta y\Delta z \tag{2.20}$$

$$f_{xB} = +\sigma_{xxB}\Delta y\Delta z \tag{2.21}$$

$$f_{xC} = -\sigma_{xyC}\Delta x\Delta z \tag{2.22}$$

$$f_{xD} = +\sigma_{xyD}\Delta x\Delta z \tag{2.23}$$

$$f_{xE} = -\sigma_{xzE}\Delta x\Delta y \tag{2.24}$$

$$f_{xF} = +\sigma_{xzF}\Delta x\Delta y \tag{2.25}$$

We replace the force Eq(2.20-2.25) to Eq (2.19):

$$(\sigma_{xxB} - \sigma_{xxA})\Delta y\Delta z + (\sigma_{xyD} - \sigma_{xyC})\Delta x\Delta z + (\sigma_{xzF} - \sigma_{xzE})\Delta x\Delta y + mg_x = ma_x \tag{2.26}$$

Normalising both sides by considered Lagrangian volume

$$V = \Delta x\Delta y\Delta z \tag{2.27}$$

we obtain

$$\frac{(\sigma_{xxB} - \sigma_{xxA})\Delta y\Delta z}{V} + \frac{(\sigma_{xyD} - \sigma_{xyC})\Delta x\Delta z}{V} + \frac{(\sigma_{xzF} - \sigma_{xzE})\Delta x\Delta y}{V} + \frac{m}{V}g_x = \frac{m}{V}a_x \tag{2.28}$$

or

$$\frac{\Delta\sigma_{xx}}{\Delta x} + \frac{\Delta\sigma_{xy}}{\Delta y} + \frac{\Delta\sigma_{xz}}{\Delta z} + \rho g_x = \rho a_x \tag{2.29}$$

doi:10.5566/NTU2018XXXXX

While the differences of the respective stresses components all tend to zero, we obtain:

$$\frac{\partial\sigma_{xx}}{\partial x}+\frac{\partial\sigma_{xy}}{\partial y}+\frac{\partial\sigma_{xz}}{\partial z}+\rho g_x=\rho a_x \tag{2.30}$$

or

$$\partial_j\sigma_{ij}+\rho g_i=\rho\ddot{u} \tag{2.31}$$

where u is the displacement.

2.1.3 Heat equation — Conservation of energy

To describe the balance of energy in a continuum material, heat equation is apply to measure the temperature change. The heat equation sloved the heat transport and porvided the temperature field. Below is the heat equation in Lagrangian form :

$$\rho C_p\frac{DT}{Dt}=-\frac{\partial q_x}{\partial x}-\frac{\partial q_y}{\partial y}-\frac{\partial q_z}{\partial z}+H_s+H_L \tag{2.32}$$

where ρ is the density, C_p is the heat capacity at constant pressure (isobaric heat capacity), H_s is shear heating and H_L is the latent heat production.

The proof of heat equation is show below:

(加上 heat equation 的推倒加圖)

Base on the Boussinesq approximation, the imcompressible Lagrangian form gov-

doi:10.5566/NTU2018XXXXX

erning equations are:

$$\nabla \cdot (\vec{v}) = 0 \frac{\partial \sigma_{ij}}{\partial x_j} + \rho g_i = \rho \frac{\partial D_{vi}}{\partial t} \rho C_p \frac{DT}{Dt} = -\frac{\partial q_x}{\partial x} - \frac{\partial q_y}{\partial y} - \frac{\partial q_z}{\partial z} + H_s + H_L \quad (2.33)$$

Describe conservation of mass, conservation of momentum and conservation of energy, respectively.

2.2 Finite elements method

finite elements method

2.3 Rheological behavior

What is viscous and the viscous rheology of rock

In the near-surface region, rocks undergo relatively low temperature and, therefore, the Earth's lithosphere easily result in brittle (at low pressure) and plastic (at high pressure) deformation. While in the deep earth, temperature increasing with depth, rocks behave viscous with irreversible deformation. Therefore, if a geodynamics model need to account for a wide range of rocks properties, it should consider the elasto-visco-plastic rheology of rocks.

Elastic rheology assume that the relationship between applied stress and strain is proportionality.

While plastic.......

doi:10.5566/NTU2018XXXXX

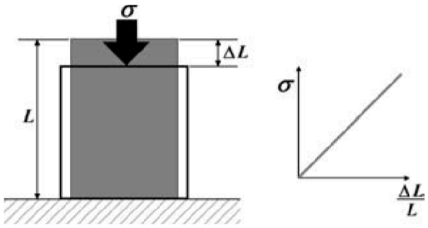

Figure 2.3: Elastic deformation

Viscous rheology define....

2.4 Phase change

In this study, we use markers to trace the rocks phases, pressure and temperature. At the time the pressure and temperature satisfy the phase transformation condition, the marker will turns to new rock phase. A basalt element represent an element with more than 30 presents of the basalt phase markers. In this case, the element behave the deformation as same as the basalt rheology.

2.4.1 Peridotite — Serpentinite

Once the subducting plate sink into mantle, sediment on oceanic plate undergo higher pressure and temperature that release a large amount of fluids. On the other hand, the oceanic plate itself also carries seawater into the mantle. Fluids in subduction zone mostly concentrated in the mantle wedge. The dry mantle wedge undergo hydration process, lead to the transformation of peridotite to serpentinite. The serpentinite depth and thickness in

doi:10.5566/NTU2018XXXXX

subduction zone is not well understand since the seismic study constrain still contain high uncertainly, we model the phase transformation process of serpentinite in parameter way.

Serpentinite are stable in the colder mantle wedge relative to deeper mantle, and therefore once the serpentinite under unstable field, we assume that serpentinite rocks release fluid and transfer to peridotite. The following equations are the conditional expressions of serpentinite—peridotite transformation. Figure is the phase diagram of mantle phases.

2.4.2 Basalt — Eclogite

As the oceanic crust sink into deeper mantle, the mafic rocks enters the eclogite stability field in the condition of high pressure. Therefore, basalt phases transform to eclogite. In this model, oceanic crust are tracked and compared with the eclogite stability filed, the following equations are the conditional expressions of mafic rocks transformation. Figure below is the mafic rocks phase diagram.

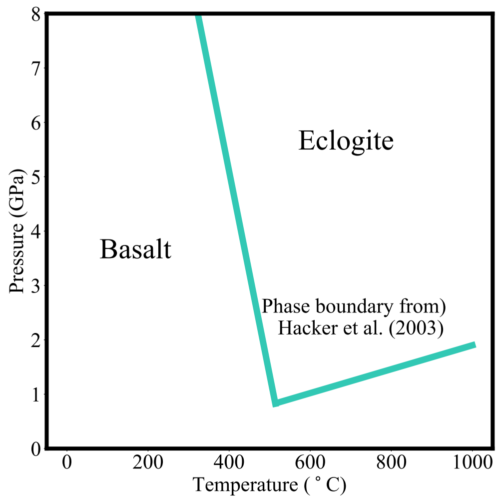

Figure 2.4: Phase diagram showing the stability field for mafic rocks (Hacker et al., 2003).

doi:10.5566/NTU2018XXXXX

2.4.3 Sediment — Schist

Once sediment undergo higher pressure, the compression process and mataphase(變質作用)process occur. In this model, the following equations are the conditional expressions of transformation process of sediment to schist.

$T > 650°C$

$depth > 20$km

The subducted sediments will turn into schist when temperature is greater than 650°C and pressure is greater than (一個數字算出來?)

2.4.4 Hydrated olivine — Peridotite

We considering a hydrated peridotite under the oceanic crust in our model. The magma will only generated above the hydrated subducting oceanic lithosphere. Once the tempertaure is too high to make the rock contain water, the hydrated olivine transform to normal perodotite. The following equation is the conditional expression of this transgformation.

$T > 800 - 35 \times 10^{-9} \times (depth - 62)^{2} °C$

doi:10.5566/NTU2018XXXXX

2.5 Boundary condition

2.5.1 Kinematic boundary condition

2.5.2 Thermal boundary condition

For oceanic lithosphere, we used half space cooling model in our model to defined the thermal condition. The plate depth is proportional to the square root of oceanic lithosphere age, and therefore, the half space cooling model can predict will for the temperature of the oceanic plate. Follow by David and Lister,1974:

$$T = T_m \cdot erf(\frac{z}{2\sqrt{\kappa t}})$$

T is the temperature, T_m is the mantle temperature, in this model the temperature is 1330, z is the depth from surface and κ is the thermal conductivity ceoficient, that is, 10^{-6} in this study. t is the lithosphere age in Myr.

For continental lithosphere, the thermal condition is defined in linearly.

2.6 FLAC

We used the Fast Lagrangian Analysis of Continua (FLAC) technique. FLAC is a two-dimensional, explicit finite element with Lagrangian gird of numerical program.

doi:10.5566/NTU2018XXXXX

2.7 Initial Model

initial model

doi:10.5566/NTU2018XXXXX

doi:10.5566/NTU2018XXXXX

Chapter 3 Numerical model result

3.1 Reference model

3.2 Flat subduction definition

3.3 Oceanic lithosphere

3.3.1 Oceanic plateau

3.3.2 Basalt transformation

3.4 Continental lithosphere

3.4.1 Thickness

3.4.2 Thermal state

3.4.3 lithosphere strength

3.5 Sublithosphere mantle

3.5.1 Viscosity

3.5.2 Serpentinization

3.5.3 410 discontinuity

doi:10.5566/NTU2018XXXXX

Chapter 4 Discussion

4.1 Type of flat subduction

4.2 Magma sources of flat subduction

4.3 Serpentinization and observation

4.4 Flat subduction in Mexico

4.5 Flat subduction in Chile

4.6 Shallow angle subduction

This is just to test [**?**] the cite function.

doi:10.5566/NTU2018XXXXX

doi:10.5566/NTU2018XXXXX

Appendix A — Introduction

A.1 Introduction

A.2 Further Introduction

doi:10.5566/NTU2018XXXXX

doi:10.5566/NTU2018XXXXX

Appendix B — Introduction

B.1 Introduction

B.2 Further Introduction

doi:10.5566/NTU2018XXXXX